HYDROLOGICAL PROCESSES
*Hydrol. Process.* **19**, 629–650 (2005)
Published online in Wiley InterScience (www.interscience.wiley.com). DOI: 10.1002/hyp.5612

# Effect of GIS data quality on small watershed stream flow and sediment simulations

Mauro Di Luzio,[1]* Jeffrey G. Arnold[2] and Raghavan Srinivasan[3]

[1] *Blackland Research Center, Texas Agricultural Experiment Station, Texas A&M University System, 720 E Blackland Rd, Temple, TX 76502, USA*
[2] *USDA-ARS, 808 E Blackland Rd, Temple, TX 76502, USA*
[3] *Spatial Sciences Laboratory, Texas A&M University, 1500 Research Parkway, Suite B223, College Station, TX 77845, USA*

## Abstract:

Simulations of total runoff and fine sediment yield in Goodwin Creek watershed, which covers 21·3 $km^2$ in Mississippi, were carried out using a hydrological model-GIS system. The system includes the recently released Soil and Water Assessment Tool (SWAT) model version 2000 and AVSWAT version 1·0, the supporting interface with ArcView GIS. Among the required GIS input, some are commonly available in the United States with multiple options and characteristics. In our study, two available digital elevation models, three land use–land cover maps and two soil maps were grouped in all possible ways to obtain 12 applied input combinations.

The objective of this study was to assess the impact of GIS input variation on the uncalibrated water runoff and sediment yield outputs and compare them with the respective observed data. The implicated issues are significant wherever multiple choices of GIS input are available. In the United States, agencies are developing TMDL (total maximum daily load) programmes at the watershed scale and are also using supporting tools along with the available GIS data. In addition, the involved water quality appraisals often include assessment of limited size watersheds, i.e. draining into a specific stream segment. This watershed, operated by the United States Department of Agriculture, Agriculture Research Service, is highly instrumented, thereby representing a severe test and a primary verification of the new system.

The GIS data had a varying impact on model results. DEM choice was critical for a realistic definition of the watershed and subwatershed boundaries and topographic input, and consequently simulated outputs. Land use–land cover maps had a significant effect on both runoff and sediment yield prediction. Soil maps showed a limited influence on model results.

While evidences and basic justifications of the results are provided, further investigations are needed to determine the influence of the input GIS data distribution on watersheds with various sizes, geomorphological and spatial settings. Copyright © 2005 John Wiley & Sons, Ltd.

KEY WORDS watershed modelling; SWAT; ArcView; GIS; water runoff; sediment yield; TMDL; watershed delineation; DEM

## INTRODUCTION

The geographical information system (GIS) is a useful technique in the development of distributed hydrologic models and in various aspects of water resources (Wilson *et al*., 2000). SWAT (Soil and Water Assessment Tool) (Arnold *et al*., 1998) is a hydrological model that greatly benefits from the GIS technology: SWAT is a watershed-based, semi-distributed hydrologic model that has been linked to GISs, such as GRASS (Srinivasan and Arnold, 1994) and ArcView (Di Luzio *et al*., 2002). The ArcView SWAT (AVSWAT) system includes several user-friendly tools that drive the user through the necessary application steps, starting with the definition

* Correspondence to: Mauro Di Luzio, Blackland Research Center, Texas Agricultural Exp Station, Texas A&M University System, 720 E Blackland Road, Temple, TX 76502 USA. E-mail: diluzio@brc.tamus.edu

*Received 16 April 2002*
*Accepted 7 May 2004*

of the watershed framework based on the topographic data (DEM) and ending with the analyses, mapping and charting of the simulation results.

The primary GIS data that must be provided are: (1) the digital elevation model; (2) the land use–land cover map; and (3) the soil map. The watershed and stream network delineation and the definition of several geomorphological parameters are calculated from the digital elevation model. The land use–land cover map defines plant classes and their distribution within each of the defined subwatersheds. The soil map provides the baseline definition of the soil classes. Jointly, these GIS layers outline and dimension the hydrologic response units (HRUs) within each subwatershed and their hydrolologic connection. Furthermore, several input parameters are initialized based on the various hydrologic aspects of HRUs in combination with model databases of plant growth, fertilizer, tillage and pesticides.

While a number of previous investigations focused mainly on watershed segmentation effects (Bingner *et al*., 1997b; FitzHugh and Mackay, 2000, 2001; Haverkamp *et al*., 2002) on SWAT model outputs, the main objective of this paper is to determine the impact of the primary GIS input layers on the model output using uniform preprocessing settings and comparing the simulated and observed runoff and sediment yields of the Goodwin Creek watershed in Mississippi. The most common, readily available GIS data are the target for this study. This uninvestigated topic, when considering the combined variation of the input, is extremely important and it is expected to unveil aspects of the simulation results neglected when using GIS-distributed model systems in support of water quality programmes. These programmes, such as the total maximum daily load (TMDL) (USEPA, 1999) currently deploying in the United States, include several water quality assessments for watersheds of small size, comparable to the case study watershed, representing the drainage area of particular stream reaches.

In addition this will be the occasion for verifying the most recent SWAT version on a small watershed provided with an outstanding set of observed water stream flow and sediment yield data along with testing the usefulness of the new AVSWAT system.

The remainder of this paper is subdivided into three sections. The first section is a short review of the SWAT model and the AVSWAT interface. The second section is a description of the case study watershed and the data used for this application. The third section is an analysis and discussion of the simulation results.

## SWAT MODEL AND AVSWAT INTERFACE

The SWAT model, version 2000, has been used in this application. This upgrade of the model has recently been developed (Arnold *et al*., 2002) with a complete review of various components of the model, including the nutrient cycle and pesticide components and the addition of new features like subdaily time step, bacteria and metal tracings. SWAT is a continuous-time model with spatially explicit parameterization. Major model components include weather, hydrology, soil temperature, plant growth, nutrients, pesticides and land management. A complete description of components can be found in Arnold *et al*. (1998). Within the simulation framework, the watershed is subdivided into subwatersheds and respective subunits with unique soil/land use characteristics (HRUs). The water balance of each HRU in the watershed is represented by four storage volumes: snow, soil profile (0–2 m), shallow aquifer (typically 2–20 m) and deep aquifer (>20 m). The soil profile can be subdivided into multiple layers. Soil water processes include infiltration, evaporation, plant uptake, lateral flow and percolation to lower layers. Flow, sediment and pollutant loading from each HRU in a subwatershed are integrated and the resulting loads are routed through channels, ponds and reservoirs to the watershed outlet.

The most recent version 1·0 of AVSWAT (ArcView-SWAT) (Di Luzio *et al*., 2002) provides a complete preprocessor, interface and postprocessor of SWAT model version 2000. AVSWAT is implemented within ArcView 3·x GIS and distributed as an extension of this software. Without leaving the ArcView 3·x GIS environment, the user applies a complete set of tools for the watershed delineation, definition and editing of the hydrological and agricultural management inputs, running and calibration of the model. AVSWAT is organized in the following eight components: (1) watershed delineation; (2) HRU definition tool; (3) editor of the model databases; (4) definition of the weather stations; (5) input parameterization and editor; (6) model run; (7) read and map–chart results; (8) calibration tool. The key types of GIS data describing the watershed landscape that must be provided are the digital elevation model, the land use–land cover map and the soil map.

## CASE STUDY WATERSHED

Goodwin Creek watershed (GCW) covers an area of 21·3 km$^2$ in the bluff hills region of the Yazoo River basin of the north central part of the state of Mississippi, just east of the flood-plain of the Mississippi River (Figure 1). Soils within GCW can generally be described as silt loams, with topography ranging from small alluvial valleys along the major channels to moderately hilly uplands. The land surface ranges in elevation from 71 to 128 m above the mean sea level, with a mean channel slope of 0·4%. The climate of GCW (USDA-ARS, 1995) is humid, hot in the summer, mild in the winter (the average daily temperature calculated for the reported years 1982–1993, and the period December–February and June–August, is around 5 °C and 27 °C, respectively). The area exhibits an annual temperature of approximately 17 °C, an average annual rainfall, measured during the period 1982–1992, of approximately 1444 mm/year. The watershed is composed entirely of rural agricultural lands (Kuhnle *et al*., 1996). There are no incorporated towns or villages in the watershed, although farm homes and rural residences are distributed throughout the area.

Since 1981, the National Sedimentation Laboratory (NSL) of the United States Department of Agriculture's Agricultural Research Service (USDA-ARS) in Oxford, MS, instrumented GCW with 14 streamflow measuring and sediment sampling stations working continuously, located through the watershed, on the outlet of one or more nested subwatersheds (Alonso *et al*., 1995), and 32 rain gauges located in or adjacent to the watershed (McGregor *et al*., 1995) recording breakpoint rainfall records. Several experimental and simulations studies have been applied to GCW (Alonso *et al*., 1995; Kuhnle *et al*., 1996; Bingner, 1996; Bingner *et al*., 1997a, b).

## GIS DATA COLLECTION

The following GIS layers (acronyms in parentheses are used later to indicate the respective data set) were collected for this study:

1. Digital elevation model
   (a) United States Geological Survey (USGS), 1 : 24 000-scale (7·5-min), spatial resolution 30 m (USGS, 1990) (*DEM 30*) in GRID format;
   (b) USGS, 1 : 250 000-scale (3-arc-sec), spatial resolution approximately 90 m (USGS, 1990) (*DEM 90*) in GRID format.
2. Land use–land cover
   (a) Map layer derived from a 1987 Landsat-5 Thematic Mapper image, spatial resolution 30 m (USDA-ARS, 1995) (*LNSL*) in GRID format;
   (b) USGS, National Land Cover Data (Vogelmann *et al*., 2001), based on 1992 vintage Landsat 5 Thematic Mapper, spatial resolution 30 m (*LNLCD*) in GRID format;
   (c) USGS, Land Use and Land Cover digital data, 1 : 250 000-scale, Level II (Anderson *et al*., 1976) (*LULC*) in shape-polygon format. Date range from 1977 to 1980.
3. Soil map
   (a) Natural Resources Conservation Service (NRCS) county soil survey map (USDA-ARS, 1995) (*SNSL*) in GRID format;
   (b) STATSGO (State Soil Geographic) Database layer (USDA-SCS, 1992), 1 : 250 000-scale soil map (*STATSGO*) in shape-polygon format.

 

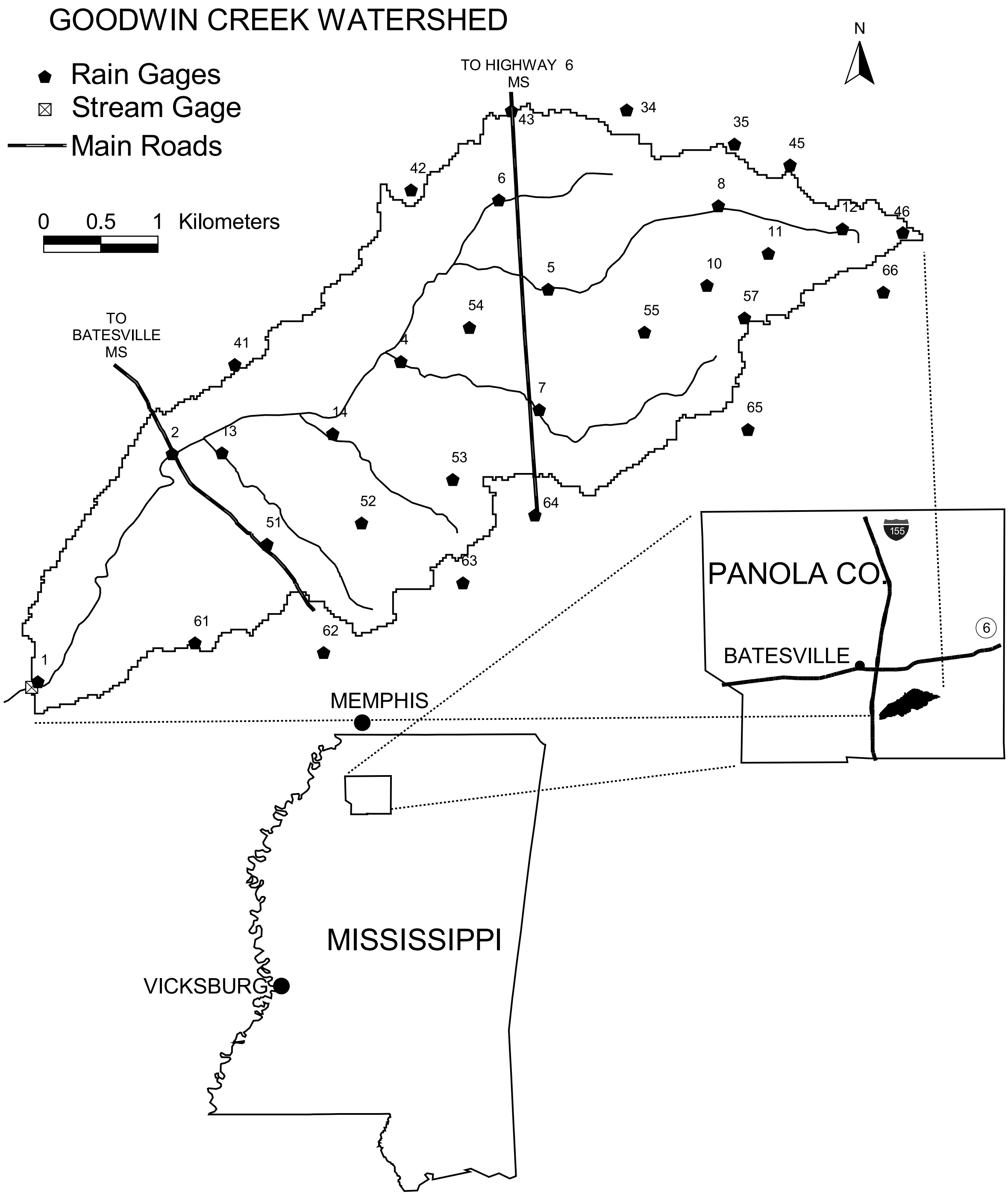


Figure 1. Location of Goodwin Creek watershed with the rain gauges and the stream flow measuring station

Except *LNSL* and *SNSL*, these are common and readily usable GIS data sets distributed by governmental agencies in the United States. Most users will broadly apply the readily available data using supporting tools (i.e. AVSWAT) for watershed water quality assessments, such as the TMDL programmes (USEPA, 1999). Other nationwide data sets, such as the National Elevation Dataset (NED) (Gesch *et al*., 2002), 30 m resolution (with 10 m resolution under development) and the Shuttle Radar Topography Mission (SRTM) (USGS, 2003) were not available at the time of this study. *LNSL, SNSL* layers were provided by the NSL. Also the SSURGO (USDA-SCS, 1994) soil map layer, becoming available for all the USA with scale generally ranging from 1 : 12 000 to 1 : 63 360, was not available for Panola County, MS, at the time of this study, but likely since county surveys are being converted to digital format (Beck *et al*., 2002), we assume it will be equivalent to the *SNSL* layer.

Before their use in AVSWAT, all these GIS layers were reported to a common coordinate system (Albers Conic Equal Area projection, North American Datum 83).

## INPUT DATA

Twelve alternative inputs, defined by the combination of the GIS layers listed above, have been used with AVSWAT (version 1·0) and SWAT (version 2000). A uniform area threshold of 100 ha was used to determine the head of the active fluvial section of the stream network. Figure 2 shows the watershed (defined with an area of 2129·67 ha), the extracted stream network using *DEM 30* and the subsequent subdivision into 248 subwatersheds defined by the outlet at each stream junction. The average size of the subwatershed was 8·59 ha, while the maximum, minimum, standard deviation and median were respectively 35·82, 0·09, 6·14 and 7·33 ha. Figure 3 shows the watershed (defined with an area of 1855·1 ha) defined using *DEM 90* with the same settings, and the subsequent subdivision into 200 subwatersheds. The average size of the subwatershed was 9·28 ha, while the maximum, minimum, standard deviation and median were respectively 77·28, 0·72, 8·61 and 7·51 ha. In both cases, the number of subwatersheds is within the range defined as optimal for this watershed and the simulations with the SWAT model (Bingner *et al*., 1997b).

The land use mapping unit distribution for GCW is shown in Tables I–III, respectively for *LNSL, LNLCD* and *LULC* maps. The watershed is dominated by pasture and forested land, while the cultivated land usage occupies most of the remaining area of the watershed.

The first two reported distributions, both for input derived from Landsat 5 data, are partially confirmed by the survey evaluations (USDA-ARS, 1995) in the same years, 1987 and 1992, respectively. Considering the surveyed pasture and idle land as a single class, their joined percentage in 1987, around 60%, matches the pasture percentage for *LNSL*, while in the surveyed assessment in 1992 it is around 10% more than for *LNLCD*. Once again the cotton class percentage in 1987 (*LNSL*) matches the surveyed percentage of cultivated area (14%). Conversely, the agriculture land in 1992 (*LNLCD*) is around 9% higher than the surveyed value. The remaining distributions of the surveyed classes, forested land and planted forested land correspond to the remote sensing interpretations when compared to the pine class in 1987 (*LNSL*) and the various forested types in 1992 (*LNLCD*). There is no way to compare the distribution of the surveyed and the *LULC* classes because dates do not match. However, the agriculture land generic class (71·9%) in *LULC* appears to include both the cultivated land and the pasture. Together, the three maps show a quite stable distribution of the forested land over time, and increasing cultivated area in 1992, although the latter is not confirmed by the surveys.

The soil mapping unit distribution for GCW is shown in Table IV and V, respectively for *SNSL* and *STATSGO* maps. Both the maps confirm that the watershed is dominated by silt soils. Soil parameters were determined linking the map units to the respective soil records elaborated using the MUUF (Map Unit User Files) method (Baumer *et al*., 1994), also used to derive the entire STATSGO-derived parameters database included in AVSWAT. Based on this elaboration, the watershed area weighted average saturated conductivity of the uppermost layer of the soil profile was 2·66 mm $h^{-1}$ and 1·29 mm $h^{-1}$ in *SNSL* and *STATSGO* cases, respectively.

 

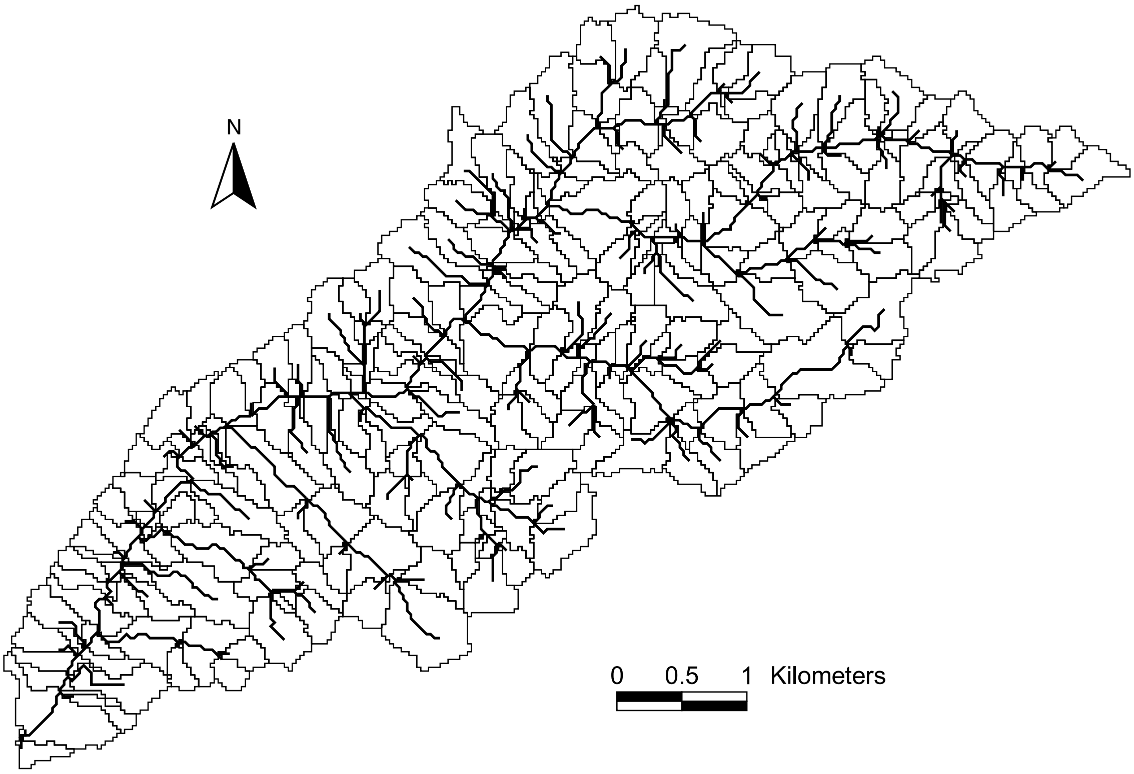


Figure 2. Subwatershed subdivisions and stream network in Goodwin Creek watershed using AVSWAT and *DEM 30* digital elevation model

The typical percentage values of 20 and 10 were used to limit the land use and soil classes within each subwatershed (Di Luzio *et al*., 2002), thus restricting the number of simulation units (HRUs). The number of HRUs, for each of the 12 input combinations, is reported in Table VI. The values range between 940 (obtained with *DEM 30–LNSL–SNSL*) and 273 (obtained with *DEM 90–LULC–STATSGO*). As expected, more detailed and larger scale inputs define a higher number of HRUs.

The SCS (Soil Conservation Service) curve number method (CN) daily rainfall data was used as an option for the simulation of surface runoff. Based on the hydrologic soil group and land use (USDA-SCS, 1972), AVSWAT assigned to each HRU the condition II curve number. Table VI reports the area weighted average value of the CN assigned to each HRU in the watershed. The following can be noted:

(a) The DEM resolution does not influence the average CN value.
(b) As far as the land use–land cover map, the average CN increases (a 1–3 range) from *LNSL* to *LNLCD*, and slightly from *LNLCD* to *LULC*.
(c) Conversely it is the large-scale soil map (*SNSL*) that determines higher (a 4–6 range) values for the average CN value.

Using an automatic procedure to analyse the entire set of input parameters, the most sensitive of them, in terms of variation within our GIS input spectrum, have been selected and added to Table VI along with their average values. The following can be noted:

(d) Obviously the average hydraulic saturated conductivity (KSAT) is shown to be independent of the land use map and the DEM resolution. The more detailed *SNSL* soil map determines an average value (around 1·75 mm $h^{-1}$) around double the value obtained using the *STATSGO* map (around 0·96 mm $h^{-1}$).

 

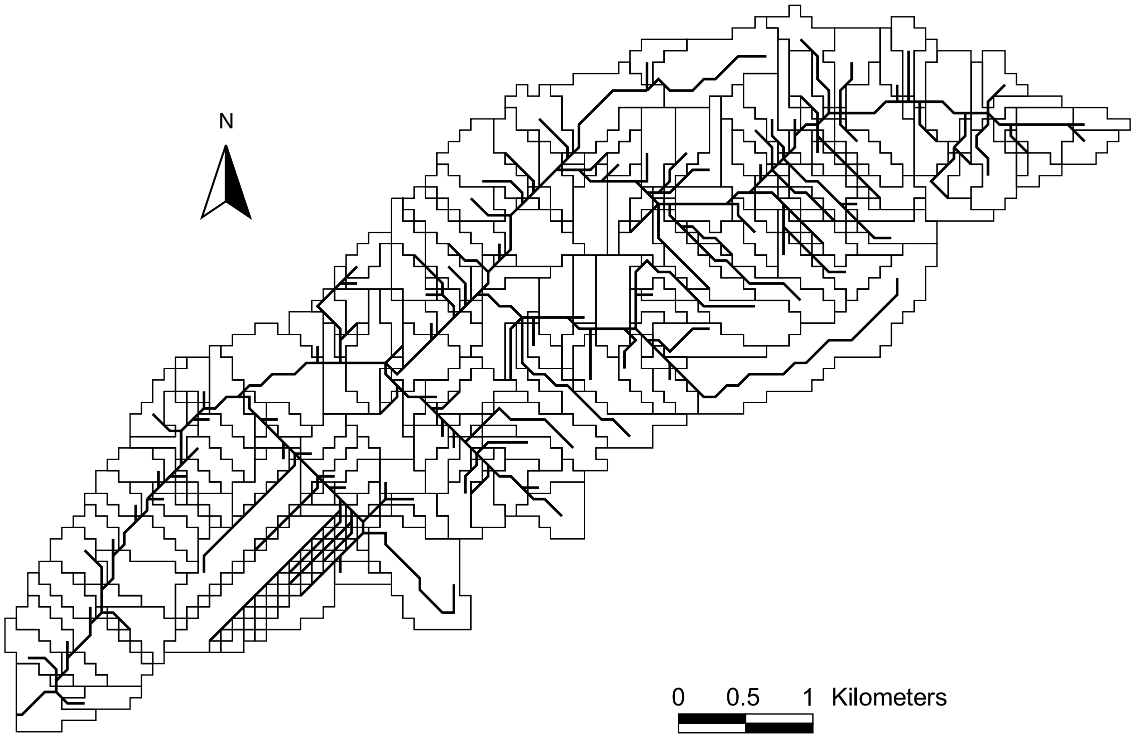


Figure 3. Subwatershed subdivisions and stream network in Goodwin Creek watershed using AVSWAT and *DEM 90* digital elevation model

Table I. Land use mapping units for Goodwin Creek watershed using *LNSL* map

| Land use | Unit extent ($km^2$) | Percentage area watershed |
|---|---|---|
| Pasture | 12·68 | 59·6 |
| Pine | 5·47 | 25·7 |
| Cotton | 3·07 | 14·4 |
| Water | 0·08 | 0·3 |

(e) Also the average available water capacity (AWC) is solely dependent upon the soil map, but conversely the higher value (around 0·22 mm $mm^{-1}$ vs around 0·196 mm $mm^{-1}$) is obtained using the STATSGO map.
(f) The erodibility factor (USLEK) is shown to be slightly dependent upon the soil map (the average value using the *STATSGO* map is slightly higher than that determined using *SNSL*).
(g) The other parameters reported in Table VI are connected to the topography of the watershed and, as expected, are highly and solely dependent upon the DEM resolution. The average slope of the subwatersheds (SLOPE) and the average channel slope (CHSLOPE) values are more than double when using *DEM 30*. Higher values of slope length (SLOPEL) and channel length (CHLEN) are obtained using *DEM 90*.

The input precipitation data set was obtained from breakpoint rainfall data collected from January 1982 to December 1993 for 31 rain gauge stations located as shown in Figure 1. The precipitation data records were

Table II. Land use mapping units for Goodwin Creek watershed using *LNLCD* map

| Land use | Unit extent ($km^2$) | Percentage area watershed |
|---|---|---|
| Pasture | 10·57 | 49·7 |
| Agricultural land-row crops | 4·55 | 21·3 |
| Forest-deciduous | 4·26 | 20·0 |
| Forest-mixed | 1·03 | 4·8 |
| Forest-evergreen | 0·70 | 3·3 |
| Water | 0·18 | 0·9 |
| Range-grasses | 0·005 | 0·02 |
| Urban-commercial | 0·004 | 0·02 |

Table III. Land use mapping units for Goodwin Creek watershed using *LULC* map

| Land use | Unit extent ($km^2$) | Percentage area watershed |
|---|---|---|
| Agricultural land-generic | 15·31 | 71·9 |
| Forest-mixed | 5·98 | 28·1 |
| Urban-transportation | 0·002 | 0·001 |

Table IV. Soil mapping units for Goodwin Creek watershed using *SNSL* map

| Soil name | Dominant texture | NRCS hydrologic soil group | Saturated conductivity upper layer ($mm\ h^{-1}$) | Unit extent ($km^2$) | Percentage area watershed |
|---|---|---|---|---|---|
| Loring | Silt | C | 1·8 | 9·59 | 45·0 |
| Collins | Silt | C | 3·3 | 3·68 | 17·3 |
| Gullied Land | Sandy loam | B | 5·0 | 3·47 | 16·3 |
| Falaya | Silt | D | 3·8 | 1·46 | 6·9 |
| Memphis | Silt | B | 1·5 | 1·38 | 6·5 |
| Grenada | Silt | C | 1·6 | 1·19 | 5·5 |
| Calloway | Silt | C | 0·65 | 0·53 | 2·5 |

Table V. Land use mapping units for Goodwin Creek watershed using *STATSGO* map

| Soil state map unit ID | Dominant texture | NRCS hydrologic soil group | Saturated conductivity upper layer ($mm\ h^{-1}$) | Unit extent ($km^2$) | Percentage area watershed |
|---|---|---|---|---|---|
| MS039 | Silt | B | 0·96 | 16·73 | 78·6 |
| MS036 | Silt | C | 2·2 | 4·54 | 21·3 |
| MS042 | Fine silt | B | 66·0 | 0·03 | 0·1 |

 

Table VI. Number of HRUs and area weighted average of selected input parameters for Goodwin Creek watershed and for each combination of input GIS data layers. CN = curve number. KSAT = saturated hydraulic conductivity. AWC = available water capacity. USLEK = universal soil loss equation soil erodibility. SLOPE = subwatershed slope. SLOPEL = slope length. CHSLOPE = slope of main channel. CHLEN = length of main channel

| DEM | Land use map | Soil map | Number of subwatersheds | Number HRUs | CN | KSAT* (mm $h^{-1}$) | AWC* (mm $mm^{-1}$) | ULSLEK 0·013 (t $m^2$ h)/($m^3$ t cm) | SLOPE (%) | SLOPEL (m) | CHSLOPE (%) | CHLEN (km) |
|---|---|---|---|---|---|---|---|---|---|---|---|---|
| *DEM 30* | *LNSL* | *SNSL 1* | 248 | 940 | 75·10 | 1·75 | 0·196 | 0·447 | 4·19 | 85·30 | 1·73 | 0·35 |
| | | *STATSGO 2* | 248 | 476 | 68·74 | 0·95 | 0·220 | 0·477 | 4·19 | 85·30 | 1·73 | 0·35 |
| | *LNLCD* | *SNSL 3* | 248 | 930 | 77·83 | 1·74 | 0·197 | 0·449 | 4·19 | 85·30 | 1·73 | 0·35 |
| | | *STATSGO 4* | 248 | 484 | 71·75 | 0·96 | 0·220 | 0·477 | 4·19 | 85·30 | 1·73 | 0·35 |
| | *LULC* | *SNSL 9* | 248 | 699 | 78·69 | 1·80 | 0·196 | 0·446 | 4·19 | 85·30 | 1·73 | 0·35 |
| | | *STATSGO 10* | 248 | 338 | 74·00 | 0·96 | 0·220 | 0·477 | 4·19 | 85·30 | 1·73 | 0·35 |
| *DEM 90* | *LNSL* | *SNSL 5* | 200 | 735 | 74·84 | 1·84 | 0·195 | 0·445 | 1·57 | 102·38 | 0·98 | 0·52 |
| | | *STATSGO 6* | 200 | 406 | 68·68 | 0·97 | 0·220 | 0·477 | 1·57 | 102·38 | 0·98 | 0·52 |
| | *LNLCD* | *SNSL 7* | 200 | 718 | 77·72 | 1·81 | 0·196 | 0·447 | 1·57 | 102·38 | 0·98 | 0·52 |
| | | *STATSGO 8* | 200 | 410 | 71·89 | 0·98 | 0·220 | 0·476 | 1·57 | 102·38 | 0·98 | 0·52 |
| | *LULC* | *SNSL 11* | 200 | 543 | 78·60 | 1·83 | 0·196 | 0·446 | 1·57 | 102·38 | 0·98 | 0·52 |
| | | *STATSGO 12* | 200 | 273 | 74·07 | 0·98 | 0·220 | 0·476 | 1·57 | 102·38 | 0·98 | 0·52 |

* This parameter is also weighted along the soil profile.

Table VII. Goodwin Creek watershed: yearly average rainfall, observed total runoff and fine sediment yield at the outlet

| Year | Average rainfall (mm) | Total runoff (mm) | Fine sediment yield (t $ha^{-1}$) |
|---|---|---|---|
| 1982 | 1692·8 | 733·5 | 17·7 |
| 1983 | 1662·3 | 864·5 | 19·6 |
| 1984 | 1447·6 | 550·9 | 16·6 |
| 1985 | 1207·8 | 309·3 | 7·5 |
| 1986 | 1235·6 | 320·3 | 5·2 |
| 1987 | 1157·9 | 317·6 | 4·2 |
| 1988 | 1053·8 | 283·0 | 3·0 |
| 1989 | 1786·3 | 846·3 | 11·9 |
| 1990 | 1482·6 | 669·6 | 9·3 |
| 1991 | 2018·9 | 1158·1 | 20·0 |
| 1992 | 1121·7 | 370·2 | 3·8 |
| 1993 | 1064·7 | 281·7 | 1·0 |
| Yearly average | 1411·00 | 558·7 | 10·0 |

arranged with a daily time step (24 h). In this study, simulated and observed stream flow and sediment yields at the watershed outlet were evaluated. The observed values of stream flow and suspended sediment load (finer than 0·062mm) sampled at the main outlet flume (the streamflow station located at 89°54′50″ and long. 34°13′55″), located as shown in Figure 1, were used in this study. Table VII reports the computed yearly average precipitation, observed total water runoff and fine sediment yield for the 12-year period January 1982 through December 1993.

With minor exceptions for sediment routing, the simulations were performed without calibration and using the default input values assigned by AVSWAT. Since most of the fine sediment at the watershed outlet originates from channel and gully sources (Grissinger *et al*., 1991), the parameter CH_EROD (channel erodibility factor) was set to 0·005 and the parameter CH_COV (channel cover factor) was set to 1·0 for each stream channel in the watershed.

The following section compares measured and simulated total runoff and fine sediment yield data for the 12-year period January 1982 through December 1993 and the 12 input combinations.

## RESULTS AND DISCUSSION

Due to the limited number of years (12) of observations, the statistical comparison of the measured and simulated total runoff and fine sediment yield data was evaluated on a monthly basis. Yearly outputs have been compared as follows.

Tables VIIIa and IXa show the simulated total runoff for each year between 1982–1993 obtained with *DEM 30* and *DEM 90* along with the combination of the other GIS inputs. Tables VIIIb and IXb show the same results as a percentage of the respective observed value. Table XIIa reports the comparison, in percentage, between the yearly runoff results obtained with *DEM 30* and *DEM 90*. The average yearly runoff prediction ranges between 73·4% (obtained with *DEM 90–LNSL–STATSGO*) and 122% (obtained with *DEM 30–LULC–SNSL*) of the respective observed value. The best result (99·2%) is obtained with the *DEM 30–LNLCD–SNSL* combination. In this case, excluding the year 1982 where the model was still 'warming up', prediction ranges between 85·9% (year 1992) and 118·9% (year 1986), not showing a correlation pattern with the yearly precipitation (i.e. wet vs dry year). The results (Table XIIa) also highlight that the thinner DEM (*DEM 30*) determines higher yearly simulated runoff values than the respective simulated values using *DEM 90*, and gaps are in a relatively quite steady ratio (around 11–13%).

 

Table VIII. (a) Observed and simulated; (b) observed and simulated (as a percentage of observed value) yearly total runoff simulation results using *DEM 30*

(a)

| Year | Observed total runoff (mm) | *LNSL SNSL* (mm) | *LNSL STATSGO* (mm) | *LNLCD SNSL* (mm) | *LNLCD STATSGO* (mm) | *LULC SNSL* (mm) | *LULC STATSGO* (mm) |
|---|---|---|---|---|---|---|---|
| 1982 | 733·5 | 506·6 | 374·6 | 529·7 | 394·5 | 656·0 | 537·6 |
| 1983 | 864·5 | 790·9 | 730·8 | 816·5 | 763·3 | 950·2 | 923·0 |
| 1984 | 550·9 | 639·7 | 590·4 | 650·8 | 608·6 | 789·4 | 770·9 |
| 1985 | 309·3 | 338·4 | 309·7 | 364·3 | 331·9 | 477·1 | 456·0 |
| 1986 | 320·3 | 345·2 | 288·0 | 380·8 | 330·4 | 521·2 | 488·8 |
| 1987 | 317·6 | 325·0 | 286·7 | 358·6 | 325·1 | 479·8 | 455·7 |
| 1988 | 283·0 | 250·3 | 203·1 | 281·5 | 240·9 | 407·9 | 382·0 |
| 1989 | 846·3 | 869·0 | 792·3 | 899·9 | 827·9 | 1058·8 | 1023·2 |
| 1990 | 669·6 | 607·6 | 561·8 | 672·7 | 632·1 | 782·7 | 750·9 |
| 1991 | 1158·1 | 1097·4 | 1023·1 | 1129·2 | 1064·5 | 1291·8 | 1253·8 |
| 1992 | 370·2 | 290·0 | 264·9 | 318·1 | 295·4 | 424·9 | 403·3 |
| 1993 | 281·7 | 215·5 | 173·6 | 246·5 | 208·2 | 377·0 | 348·4 |
| Yearly average | 558·7 | 523·0 | 466·6 | 554·1 | 501·9 | 684·7 | 649·5 |

(b)

| Year | Observed total runoff (mm) | *LNSL SNSL* (%) | *LNSL STATSGO* (%) | *LNLCD SNSL* (%) | *LNLCD STATSGO* (%) | *LULC SNSL* (%) | *LULC STATSGO* (%) |
|---|---|---|---|---|---|---|---|
| 1982 | 733·5 | 69·1 | 51·1 | 72·2 | 53·8 | 89·4 | 73·3 |
| 1983 | 864·5 | 91·5 | 84·5 | 94·4 | 88·3 | 109·9 | 106·8 |
| 1984 | 550·9 | 116·1 | 107·2 | 118·1 | 110·5 | 143·3 | 139·9 |
| 1985 | 309·3 | 109·4 | 100·1 | 117·8 | 107·3 | 154·3 | 147·4 |
| 1986 | 320·3 | 107·8 | 89·9 | 118·9 | 103·2 | 162·7 | 152·6 |
| 1987 | 317·6 | 102·3 | 90·3 | 112·9 | 102·4 | 151·1 | 143·5 |
| 1988 | 283·0 | 88·4 | 71·8 | 99·5 | 85·1 | 144·1 | 135·0 |
| 1989 | 846·3 | 102·7 | 93·6 | 106·3 | 97·8 | 125·1 | 120·9 |
| 1990 | 669·6 | 90·7 | 83·9 | 100·5 | 94·4 | 116·9 | 112·1 |
| 1991 | 1158·1 | 94·8 | 88·3 | 97·5 | 91·9 | 111·5 | 108·3 |
| 1992 | 370·2 | 78·3 | 71·6 | 85·9 | 79·8 | 114·8 | 108·9 |
| 1993 | 281·7 | 76·5 | 61·6 | 87·5 | 73·9 | 133·8 | 123·7 |
| Yearly average | 558·7 | 93·6 | 83·5 | 99·2 | 89·8 | 122·6 | 116·3 |

Tables Xa and XIa show the simulated fine sediment yield for each year between 1982–1993 obtained with *DEM 30* and *DEM 90* along with the combination of the other GIS inputs. Tables Xb and XIb show the same results as a percentage of the respective observed value. Table XIIb reports the comparison, in percentage, between the yearly sediment yield results obtained with *DEM 30* and *DEM 90*. The average yearly sediment yield prediction ranges parallel the runoff predictions: 77% (obtained with *DEM 90–LNSL–STATSGO*) and 456% (obtained with *DEM 30–LULC–SNSL*) of the respective observed value. In turn the best result (99·0%) is obtained with the *DEM 90–LNLCD–STATSGO* combination. In this case, excluding the year 1982 where the model was still 'warming up', prediction ranges between 71·1% (year 1984) and 400·0% (year 1993). The general overprediction is justified since the observed data are only the portion of fine sediment (<0·062 mm) while the model estimates the entire load. The results (Table XIIb) also highlight that the thinner DEM (*DEM 30*) determines remarkably high yearly simulated sediment values, and gaps with the respective simulated

 

Table IX. (a) Observed and simulated; (b) observed and simulated (as a percentage of observed value) yearly total runoff results using *DEM 90*

(a)

| Year | Observed total runoff (mm) | *LNSL SNSL* (mm) | *LNSL STATSGO* (mm) | *LNLCD SNSL* (mm) | *LNLCD STATSGO* (mm) | *LULC SNSL* (mm) | *LULC STATSGO* (mm) |
|---|---|---|---|---|---|---|---|
| 1982 | 733·5 | 447·2 | 335·0 | 464·7 | 350·4 | 568·7 | 471·0 |
| 1983 | 864·5 | 693·9 | 642·2 | 713·3 | 668·3 | 824·7 | 802·7 |
| 1984 | 550·9 | 562·9 | 519·9 | 569·3 | 533·4 | 684·1 | 669·7 |
| 1985 | 309·3 | 297·8 | 273·6 | 319·7 | 292·3 | 414·2 | 396·9 |
| 1986 | 320·3 | 305·2 | 256·4 | 335·1 | 293·6 | 452·7 | 426·1 |
| 1987 | 317·6 | 287·3 | 253·7 | 316·0 | 287·9 | 417·0 | 396·5 |
| 1988 | 283·0 | 222·6 | 181·5 | 248·9 | 214·6 | 354·1 | 332·3 |
| 1989 | 846·3 | 761·3 | 697·2 | 784·5 | 725·1 | 918·6 | 888·5 |
| 1990 | 669·6 | 525·3 | 486·5 | 583·8 | 551·3 | 676·6 | 650·7 |
| 1991 | 1158·1 | 954·5 | 889·2 | 979·2 | 922·9 | 1115·4 | 1082·2 |
| 1992 | 370·2 | 254·9 | 232·2 | 279·7 | 259·9 | 369·9 | 350·9 |
| 1993 | 281·7 | 191·3 | 154·3 | 218·4 | 185·6 | 328·4 | 304·3 |
| Yearly average | 558·7 | 458·7 | 410·1 | 484·4 | 440·4 | 593·7 | 564·3 |

(b)

| Year | Observed total runoff (mm) | *LNSL SNSL* (%) | *LNSL STATSGO* (%) | *NLCD SNSL* (%) | *NLCD STATSGO* (%) | *LULC SNSL* (%) | *LULC STATSGO* (%) |
|---|---|---|---|---|---|---|---|
| 1982 | 733·5 | 61·0 | 45·7 | 63·4 | 47·8 | 77·5 | 64·2 |
| 1983 | 864·5 | 80·3 | 74·3 | 82·5 | 77·3 | 95·4 | 92·9 |
| 1984 | 550·9 | 102·2 | 94·4 | 103·3 | 96·8 | 124·2 | 121·6 |
| 1985 | 309·3 | 96·3 | 88·5 | 103·4 | 94·5 | 133·9 | 128·3 |
| 1986 | 320·3 | 95·3 | 80·0 | 104·6 | 91·7 | 141·3 | 133·0 |
| 1987 | 317·6 | 90·5 | 79·9 | 99·5 | 90·6 | 131·3 | 124·8 |
| 1988 | 283·0 | 78·7 | 64·1 | 88·0 | 75·8 | 125·1 | 117·4 |
| 1989 | 846·3 | 90·0 | 82·4 | 92·7 | 85·7 | 108·5 | 105·0 |
| 1990 | 669·6 | 78·4 | 72·7 | 87·2 | 82·3 | 101·0 | 97·2 |
| 1991 | 1158·1 | 82·4 | 76·8 | 84·6 | 79·7 | 96·3 | 93·4 |
| 1992 | 370·2 | 68·9 | 62·7 | 75·6 | 70·2 | 99·9 | 94·8 |
| 1993 | 281·7 | 67·9 | 54·8 | 77·5 | 65·9 | 116·6 | 108·0 |
| Yearly average | 558·7 | 82·1 | 73·4 | 86·7 | 78·8 | 106·3 | 101·0 |

values using *DEM 90* are in a relatively quite steady ratio modulated by the land use map: around 39·5% using *LNSL*, 47·5% using *NLCD* and 55% using *LULC*.

The monthly average water yield, observed at the watershed outlet during the evaluation period, was 46·56 mm (standard deviation 62·45 mm). The statistical analysis of the simulated versus observed total monthly runoff is reported for each of the 12 simulations in Table XIII. The plots of the monthly simulations versus the observed values for the best and worst combinations are reported in Figures 4 and 5, respectively. In general the model provides a good estimate of the monthly runoff, particularly the lower values, while the higher values tend to be underestimated. The model efficiency ($E$) (Nash and Sutcliffe, 1970) varies between 0·97 (obtained with *DEM 30–LNLCD–SNSL*, best combination also for the yearly results) and 0·81 (*DEM 90–LNSL–STATSGO*, worst combination also for the yearly lowest average result). In addition, the following can be noted:

 

Table X. (a) Observed and simulated; (b) observed and simulated (as a percentage of observed value) yearly fine sediment yield results using *DEM 30*

(a)

| Year | Observed fine sediment yield (t $ha^{-1}$) | *LNSL SNSL* (t $ha^{-1}$) | *LNSL STATSGO* (t $ha^{-1}$) | *NLCD SNSL* (t $ha^{-1}$) | *NLCD STATSGO* (t $ha^{-1}$) | *LULC SNSL* (t $ha^{-1}$) | *LULC STATSGO* (t $ha^{-1}$) |
|---|---|---|---|---|---|---|---|
| 1982 | 17·7 | 16·8 | 11·9 | 21·8 | 18·0 | 48·9 | 43·1 |
| 1983 | 19·6 | 22·9 | 21·6 | 30·9 | 29·7 | 67·2 | 66·1 |
| 1984 | 16·6 | 17·4 | 16·5 | 23·6 | 22·8 | 53·1 | 53·1 |
| 1985 | 7·5 | 8·4 | 7·8 | 15·1 | 14·2 | 35·3 | 33·6 |
| 1986 | 5·2 | 9·5 | 7·7 | 15·3 | 14·4 | 38·5 | 37·0 |
| 1987 | 4·2 | 8·0 | 6·9 | 13·4 | 12·7 | 32·5 | 31·9 |
| 1988 | 3·0 | 5·7 | 4·3 | 9·7 | 8·2 | 23·5 | 21·3 |
| 1989 | 11·9 | 26·3 | 25·6 | 33·8 | 33·4 | 77·4 | 77·8 |
| 1990 | 9·3 | 13·4 | 12·2 | 20·3 | 19·1 | 44·0 | 42·3 |
| 1991 | 20·0 | 27·0 | 25·6 | 35·2 | 35·1 | 75·3 | 76·1 |
| 1992 | 3·8 | 8·5 | 8·0 | 12·6 | 12·0 | 29·7 | 27·6 |
| 1993 | 1·0 | 5·3 | 4·1 | 9·0 | 7·8 | 21·8 | 20·1 |
| Yearly average | 10·0 | 14·1 | 12·7 | 20·1 | 18·9 | 45·6 | 44·2 |

(b)

| Year | Observed fine sediment yield (t $ha^{-1}$) | *LNSL SNSL* (%) | *LNSL STATSGO* (%) | *NLCD SNSL* (%) | *NLCD STATSGO* (%) | *LULC SNSL* (%) | *LULC STATSGO* (%) |
|---|---|---|---|---|---|---|---|
| 1982 | 17·7 | 94·9 | 67·2 | 123·2 | 101·7 | 276·3 | 243·5 |
| 1983 | 19·6 | 116·8 | 110·2 | 157·7 | 151·5 | 342·9 | 337·2 |
| 1984 | 16·6 | 104·8 | 99·4 | 142·2 | 137·3 | 319·9 | 319·9 |
| 1985 | 7·5 | 112·0 | 104·0 | 201·3 | 189·3 | 470·7 | 448·0 |
| 1986 | 5·2 | 182·7 | 148·1 | 294·2 | 276·9 | 740·4 | 711·5 |
| 1987 | 4·2 | 190·5 | 164·3 | 319·0 | 302·4 | 773·8 | 759·5 |
| 1988 | 3·0 | 190·0 | 143·3 | 323·3 | 273·3 | 783·3 | 710·0 |
| 1989 | 11·9 | 221·0 | 215·1 | 284·0 | 280·7 | 650·4 | 653·8 |
| 1990 | 9·3 | 144·1 | 131·2 | 218·3 | 205·4 | 473·1 | 454·8 |
| 1991 | 20·0 | 135·0 | 128·0 | 176·0 | 175·5 | 376·5 | 380·5 |
| 1992 | 3·8 | 223·7 | 210·5 | 331·6 | 315·8 | 781·6 | 726·3 |
| 1993 | 1·0 | 530·0 | 410·0 | 900·0 | 780·0 | 2180·0 | 2010·0 |
| Yearly average | 10·0 | 141·0 | 127·0 | 201·0 | 189·0 | 456·0 | 442·0 |

(i) Coarser DEM (*DEM 90* vs *DEM 30*) with the same land use and soil map generally renders an increased underestimation along with a decrease of *E*. The exceptions are determined with *SNSL* and the *LULC* map. These results, along with the steady ratio between the yearly results obtained with the two topography settings noted above, can be explained taking into account points (a) average CN invariance, (d) KSAT invariance and (e) AWC invariance highlighted in the previous section along with the fact that *DEM 90* also resulted in an inaccurate and poorly defined watershed and subwatersheds boundary, as shown in Figure 3. In fact, the relative difference in watershed area (11–13%) resembles the difference in the yearly simulated runoff using the two DEMs. Finally, *DEM 90* contributes to lower the already underestimated results obtained with *DEM 30*. The exception is explained by point (ii) below. The combination *DEM 30–LULC–SNLS* results in a slight overestimation.

 

Table XI. (a) Observed and simulated; (b) observed and simulated (as a percentage of observed value) yearly fine sediment yield results using *DEM 90*

(a)

| Year | Observed fine sediment yield (t ha$^{-1}$) | *LNSL SNSL* (t ha$^{-1}$) | *LNSL STATSGO* (t ha$^{-1}$) | *NLCD SNSL* (t ha$^{-1}$) | *NLCD STATSGO* (t ha$^{-1}$) | *LULC SNSL* (t ha$^{-1}$) | *LULC STATSGO* (t ha$^{-1}$) |
|---|---|---|---|---|---|---|---|
| 1982 | 17·7 | 9·6 | 7·1 | 11·7 | 9·5 | 22·3 | 20·0 |
| 1983 | 19·6 | 13·6 | 12·8 | 16·3 | 15·5 | 29·7 | 30·5 |
| 1984 | 16·6 | 10·6 | 10·0 | 12·5 | 11·8 | 23·3 | 24·4 |
| 1985 | 7·5 | 5·0 | 4·6 | 7·7 | 7·1 | 15·6 | 15·7 |
| 1986 | 5·2 | 5·9 | 4·8 | 7·9 | 7·2 | 16·7 | 16·9 |
| 1987 | 4·2 | 4·8 | 4·1 | 7·0 | 6·4 | 13·9 | 14·0 |
| 1988 | 3·0 | 3·5 | 2·6 | 5·1 | 4·3 | 10·3 | 9·6 |
| 1989 | 11·9 | 16·0 | 15·3 | 17·6 | 17·0 | 33·7 | 35·2 |
| 1990 | 9·3 | 8·3 | 7·5 | 11·2 | 10·6 | 19·8 | 19·3 |
| 1991 | 20·0 | 16·8 | 15·9 | 19·4 | 18·9 | 33·9 | 35·3 |
| 1992 | 3·8 | 5·0 | 4·7 | 6·4 | 6·0 | 13·2 | 13·1 |
| 1993 | 1·0 | 3·2 | 2·4 | 4·7 | 4·0 | 9·6 | 9·0 |
| Yearly average | 10·0 | 8·5 | 7·7 | 10·6 | 9·9 | 20·2 | 20·3 |

(b)

| Year | Observed fine sediment yield (t ha$^{-1}$) | *LNSL SNSL* (%) | *LNSL STATSGO* (%) | *NLCD SNSL* (%) | *NLCD STATSGO* (%) | *LULC SNSL* (%) | *LULC STATSGO* (%) |
|---|---|---|---|---|---|---|---|
| 1982 | 17·7 | 54·2 | 40·1 | 66·1 | 53·7 | 126·0 | 113·0 |
| 1983 | 19·6 | 69·4 | 65·3 | 83·2 | 79·1 | 151·5 | 155·6 |
| 1984 | 16·6 | 63·9 | 60·2 | 75·3 | 71·1 | 140·4 | 147·0 |
| 1985 | 7·5 | 66·7 | 61·3 | 102·7 | 94·7 | 208·0 | 209·3 |
| 1986 | 5·2 | 113·5 | 92·3 | 151·9 | 138·5 | 321·2 | 325·0 |
| 1987 | 4·2 | 114·3 | 97·6 | 166·7 | 152·4 | 331·0 | 333·3 |
| 1988 | 3·0 | 116·7 | 86·7 | 170·0 | 143·3 | 343·3 | 320·0 |
| 1989 | 11·9 | 134·5 | 128·6 | 147·9 | 142·9 | 283·2 | 295·8 |
| 1990 | 9·3 | 89·2 | 80·6 | 120·4 | 114·0 | 212·9 | 207·5 |
| 1991 | 20·0 | 84·0 | 79·5 | 97·0 | 94·5 | 169·5 | 176·5 |
| 1992 | 3·8 | 131·6 | 123·7 | 168·4 | 157·9 | 347·4 | 344·7 |
| 1993 | 1·0 | 320·0 | 240·0 | 470·0 | 400·0 | 960·0 | 900·0 |
| Yearly average | 10·0 | 85·0 | 77·0 | 106·0 | 99·0 | 202·0 | 203·0 |

(ii) Using a coarser land use map (*LULC*) with the same DEM and soil map generally renders an improvement in the runoff estimation, except for the *DEM 30–SNSL* combination. This result can be explained taking into account point (b) highlighted in the previous section (increase in average CN). The basic underestimation of the model for this watershed is improved by this factor providing higher runoff.

(iii) Using a coarser soil map (*STATSGO*) with the same DEM and land use map results in lower runoff values obtained using the *SNSL* with slight deteriorating influence on the statistical results. This result can be explained taking into account points (c) average decrease of CN, (d) average decrease of KSAT and (e) average increase of AWC highlighted in the previous section. The first factor, once again, contributes to lower the already underestimated outputs, while the other two factors could have an influence in undefined and inconsistent directions.

 

Table XII. Difference of (a) simulated total runoff results; (b) simulated fine sediment yields using *DEM 30* and *DEM 90* as a percentage of the values obtained using *DEM 30*

(a)

| Year | Observed total runoff (mm) | *LNSL SNSL* (%) | *LNSL STATSGO* (%) | *NLCD SNSL* (%) | *NLCD STATSGO* (%) | *LULC SNSL* (%) | *LULC STATSGO* (%) |
|---|---|---|---|---|---|---|---|
| 1982 | 733·5 | 11·7 | 10·6 | 12·3 | 11·2 | 13·3 | 12·4 |
| 1983 | 864·5 | 12·3 | 12·1 | 12·6 | 12·4 | 13·2 | 13·0 |
| 1984 | 550·9 | 12·0 | 11·9 | 12·5 | 12·4 | 13·3 | 13·1 |
| 1985 | 309·3 | 12·0 | 11·7 | 12·2 | 11·9 | 13·2 | 13·0 |
| 1986 | 320·3 | 11·6 | 11·0 | 12·0 | 11·1 | 13·1 | 12·8 |
| 1987 | 317·6 | 11·6 | 11·5 | 11·9 | 11·4 | 13·1 | 13·0 |
| 1988 | 283·0 | 11·1 | 10·6 | 11·6 | 10·9 | 13·2 | 13·0 |
| 1989 | 846·3 | 12·4 | 12·0 | 12·8 | 12·4 | 13·2 | 13·2 |
| 1990 | 669·6 | 13·5 | 13·4 | 13·2 | 12·8 | 13·6 | 13·3 |
| 1991 | 1158·1 | 13·0 | 13·1 | 13·3 | 13·3 | 13·7 | 13·7 |
| 1992 | 370·2 | 12·1 | 12·3 | 12·1 | 12·0 | 12·9 | 13·0 |
| 1993 | 281·7 | 11·2 | 11·1 | 11·4 | 10·9 | 12·9 | 12·7 |
| Yearly average | 558·7 | 12·3 | 12·1 | 12·6 | 12·3 | 13·3 | 13·1 |

(b)

| Year | Observed fine sediment yield (t $ha^{-1}$) | *LNSL SNSL* (%) | *LNSL STATSGO* (%) | *NLCD SNSL* (%) | *NLCD STATSGO* (%) | *LULC SNSL* (%) | *LULC STATSGO* (%) |
|---|---|---|---|---|---|---|---|
| 1982 | 17·7 | 42·9 | 40·3 | 46·3 | 47·2 | 54·4 | 53·6 |
| 1983 | 19·6 | 40·6 | 40·7 | 47·2 | 47·8 | 55·8 | 53·9 |
| 1984 | 16·6 | 39·1 | 39·4 | 47·0 | 48·2 | 56·1 | 54·0 |
| 1985 | 7·5 | 40·5 | 41·0 | 49·0 | 50·0 | 55·8 | 53·3 |
| 1986 | 5·2 | 37·9 | 37·7 | 48·4 | 50·0 | 56·6 | 54·3 |
| 1987 | 4·2 | 40·0 | 40·6 | 47·8 | 49·6 | 57·2 | 56·1 |
| 1988 | 3·0 | 38·6 | 39·5 | 47·4 | 47·6 | 56·2 | 54·9 |
| 1989 | 11·9 | 39·2 | 40·2 | 47·9 | 49·1 | 56·5 | 54·8 |
| 1990 | 9·3 | 38·1 | 38·5 | 44·8 | 44·5 | 55·0 | 54·4 |
| 1991 | 20·0 | 37·8 | 37·9 | 44·9 | 46·2 | 55·0 | 53·6 |
| 1992 | 3·8 | 41·2 | 41·3 | 49·2 | 50·0 | 55·6 | 52·5 |
| 1993 | 1·0 | 39·6 | 41·5 | 47·8 | 48·7 | 56·0 | 55·2 |
| Yearly average | 10·0 | 39·7 | 39·4 | 47·3 | 47·6 | 55·7 | 54·1 |

The monthly average sediment yield, observed at the watershed outlet during the evaluation period, was 0·83 t $ha^{-1}$ (standard deviation 1·51 t $ha^{-1}$). The statistical analysis of the simulated versus observed monthly fine sediment yield is reported for each of the 12 simulations in Table XIV. The plots of the monthly simulations versus the observed values for the best and worst combinations are reported in Figures 6 and 7, respectively. In general the model provides estimates of the monthly sediment yield with a high degree of variability.

$E$ varies between 0·70 (obtained with *DEM 90–LNCD–SNSL*) and −8·21 (obtained with *DEM 30–LULC–SNSL*). In addition, recalling that the observed data are only the portion of fine sediment (<0·062 mm) while the model estimates the entire load (this issue in the remainder of the paper will be referenced as 'the fine sediment issue'):

 

Table XIII. Statistical parameters* from monthly observed vs simulated surface total runoff using SWAT–AVSWAT with different input GIS data sets for the period January 1982–December 1993

| DEM | Land use map | | | Soil map |
|---|---|---|---|---|
| | *LNSL* | *LNLCD* | *LULC* | |
| *DEM 30* | Mean = 43·58<br>SD = 54·66<br>$E = 0{\cdot}93$<br>Slope = 0·85<br>Intercept = 4·10<br>$R^2 = 0{\cdot}94$ | Mean = 46·17<br>SD = 57·45<br>$E = 0{\cdot}97$<br>Slope = 0·89<br>Intercept = 4·49<br>$R^2 = 0{\cdot}95$ | Mean = 57·06<br>SD = 61·50<br>$E = 0{\cdot}91$<br>Slope = 0·95<br>Intercept = 12·54<br>$R^2 = 0{\cdot}94$ | *SNSL* |
| | Mean = 38·88<br>SD = 50·68<br>$E = 0{\cdot}87$<br>Slope = 0·77<br>Intercept = 3·02<br>$R^2 = 0{\cdot}90$ | Mean = 41·8<br>SD = 53·84<br>$E = 0{\cdot}90$<br>Slope = 0·82<br>Intercept = 3·45<br>$R^2 = 0{\cdot}91$ | Mean = 54·12<br>SD = 59·53<br>$E = 0{\cdot}91$<br>Slope = 0·91<br>Intercept = 11·4<br>$R^2 = 0{\cdot}92$ | *STATSGO* |
| *DEM 90* | Mean = 38·22<br>SD = 47·24<br>$E = 0{\cdot}88$<br>Slope = 0·73<br>Intercept = 4·09<br>$R^2 = 0{\cdot}94$ | Mean = 40·36<br>SD = 49·75<br>$E = 0{\cdot}91$<br>Slope = 0·78<br>Intercept = 4·25<br>$R^2 = 0{\cdot}95$ | Mean = 49·48<br>SD = 53·30<br>$E = 0{\cdot}93$<br>Slope = 0·82<br>Intercept = 10·92<br>$R^2 = 0{\cdot}94$ | *SNSL* |
| | Mean = 34·17<br>SD = 44·02<br>$E = 0{\cdot}81$<br>Slope = 0·61<br>Intercept = 3·00<br>$R^2 = 0{\cdot}90$ | Mean = 36·7<br>SD = 46·91<br>$E = 0{\cdot}85$<br>Slope = 0·72<br>Intercept = 3·24<br>$R^2 = 0{\cdot}92$ | Mean = 47·02<br>SD = 51·70<br>$E = 0{\cdot}91$<br>Slope = 0·80<br>Intercept = 9·96<br>$R^2 = 0{\cdot}92$ | *STATSGO* |

* Mean is the average and SD is the standard deviation of the simulated, monthly values. $E$ is the Nash and Sutcliffe (1970) model efficiency. Slope and Intercept follow from the linear regression between observed and simulated monthly values. $R^2$ is the coefficient of determination.

(iv) Using a coarser DEM (*DEM 90* vs *DEM 30*) with the same land use and soil map generally renders an improvement in the results. These results can be explained taking into account two concurrent factors: the first includes the issue highlighted in point (i) of this section and the topographic characteristics highlighted in point (g) of the previous section, both causing lower sediment predictions using *DEM 90* when compared to those obtained using *DEM 30;* the second is 'the fine sediment issue'. The land use map modulates the discrepancy between the simulations using *DEM 30* and *DEM 90* as a consequence of the USLE crop factor that is simulated by the model, paralleling the percentage of cultivated land in the three map cases.

(v) Use of a coarser land use map (*LULC*) with the same DEM and soil map generally causes a considerable overestimation. Land use maps bias the simulations, including the yearly difference ratios between *DEM 90* and *DEM 30* results (Table XIIb), regardless of the soil map used. This effect can be explained taking into account point (ii) of this section. The higher simulated runoff determines a consequent increased erosion estimate.

(vi) Use of a coarser soil map (*STATSGO*) with the same DEM and land use map generally has a very limited impact on the same estimates using *SNSL*. This effect can be explained taking into account once again 'the fine sediment issue' and counteracting compensating factors: part of these factors are highlighted within point (iii) of this section (decrease of runoff); the remainder is highlighted in point (f) higher average USLEK of the previous section.

 

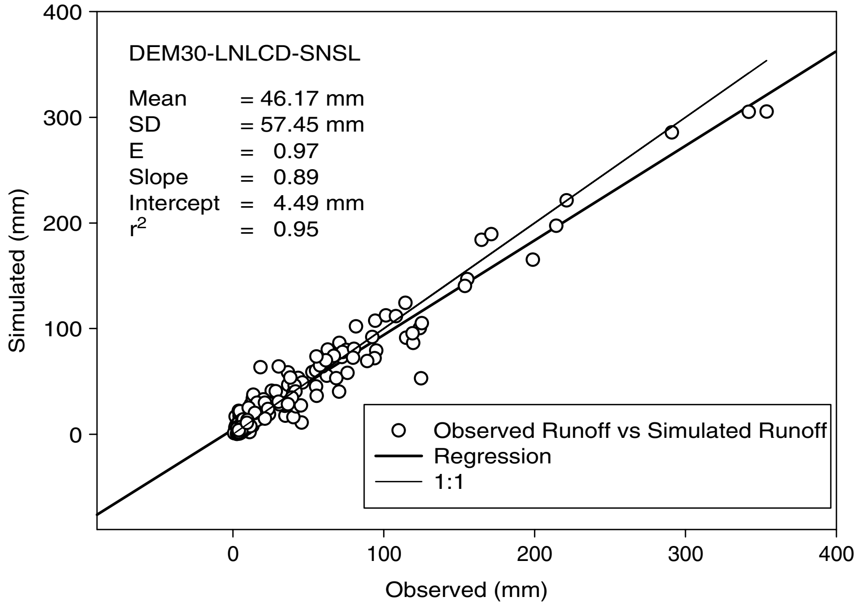


Figure 4. Observed and simulated monthly runoff using the GIS input: *DEM 30–LNLCD–SNLS*

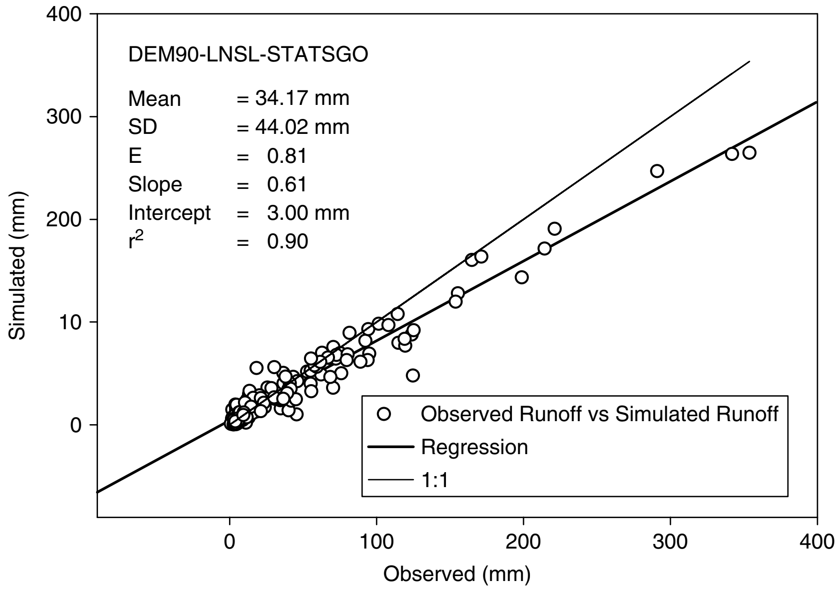


Figure 5. Observed and simulated monthly runoff using the GIS input: *DEM 90–LNSL–STATSGO*

A test of the new AVSWAT system was desired to verify its basic reliability and user support functionality. The results of the embedded SWAT model version 2000, described above, are quite reasonable and similar to those obtained with earlier versions of the model, different GIS systems and settings (Bingner, 1996; Bingner *et al*., 1997a, b). Specifically, the ArcView GIS interface, in addition to its user-friendliness that shields users from the GIS core complexity, provided full control and ability to interchange various GIS input data with different formats and properties.

 

Table XIV. Statistical parameters* from monthly observed vs simulated fine sediment yield using SWAT–AVSWAT with different input GIS data sets for the period January 1982–December 1993

| DEM | Land use map | | | Soil Map |
|---|---|---|---|---|
| | *LNSL* | *LNLCD* | *LULC* | |
| *DEM 30* | Mean = 1·17<br>SD = 1·59<br>$E$ = 0·61<br>Slope = 0·89<br>Intercept = 0·44<br>$R^2$ = 0·71 | Mean = 1·67<br>SD = 2·04<br>$E$ = 0·12<br>Slope = 1·13<br>Intercept = 0·73<br>$R^2$ = 0·69 | Mean = 3·80<br>SD = 4·6<br>$E$ = −8·21<br>Slope = 2·43<br>Intercept = 1·78<br>$R^2$ = 0·64 | *SNSL* |
| | Mean = 1·06<br>SD = 1·54<br>$E$ = 0·62<br>Slope = 0·84<br>Intercept = 0·36<br>$R^2$ = 0·68 | Mean = 1·58<br>SD = 2·03<br>$E$ = 0·17<br>Slope = 1·11<br>Intercept = 0·65<br>$R^2$ = 0·68 | Mean = 3·68<br>SD = 4·66<br>$E$ = −8·13<br>Slope = 2·43<br>Intercept = 1·66<br>$R^2$ = 0·62 | *STATSGO* |
| *DEM 90* | Mean = 0·71<br>SD = 0·97<br>$E$ = 0·66<br>Slope = 0·54<br>Intercept = 0·26<br>$R^2$ = 0·70 | Mean = 0·88<br>SD = 1·10<br>$E$ = 0·70<br>Slope = 0·61<br>Intercept = 0·38<br>$R^2$ = 0·71 | Mean = 1·68<br>SD = 2·02<br>$E$ = 0·08<br>Slope = 1·09<br>Intercept = 0·77<br>$R^2$ = 0·66 | *SNSL* |
| | Mean = 0·64<br>SD = 0·93<br>$E$ = 0·63<br>Slope = 0·51<br>Intercept = 0·21<br>$R^2$ = 0·68 | Mean = 0·82<br>SD = 1·07<br>$E$ = 0·68<br>Slope = 0·59<br>Intercept = 0·33<br>$R^2$ = 0·69 | Mean = 1·69<br>SD = 2·14<br>$E$ = −0·05<br>Slope = 1·14<br>Intercept = 0·74<br>$R^2$ = 0·64 | *STATSGO* |

* Mean is the average and SD is the standard deviation of the simulated, monthly values. $E$ is the Nash and Sutcliffe (1970) model efficiency. Slope and Intercept follow from the linear regression between observed and simulated monthly values. $R^2$ is the coefficient of determination.

However, the main objective of the study was to highlight the implications, on hydrologic simulations, of using a particular input GIS data set when a number of options are available. This has more recently become a stringent issue, whereas in the past, and still in most countries, input options are more limited. In the United States, the potential positive proliferation of GIS data developed by governmental agencies and available at no cost poses increasing uncertainty in the consequences and appropriateness of using one data set rather than another. In addition, the case study is a small watershed representing the typical size of a number of water quality assessments (i.e. TMDL), which are also often ungauged, thereby justifying our comparison of uncalibrated simulations.

In our study, the variations of simulation and GIS input preprocessing and preparation time were irrelevant due to the size of the watershed. The results of the various organized simulations for this watershed demonstrated:

1. The coarsest DEM (*DEM 90*) affected the delineation results (watershed and subwatershed boundary as well as dimensioning some geomorphological parameters) significantly. The erroneous calculation of the watershed area has a direct impact on runoff and consequently on sediment yield outputs. In addition, both the watershed area and geomorphological parameters assume values that concurrently contribute to decrease soil erosion and sediment yield, thereby improving $E$. However, this is mainly connected to 'the fine sediment issue'.

 

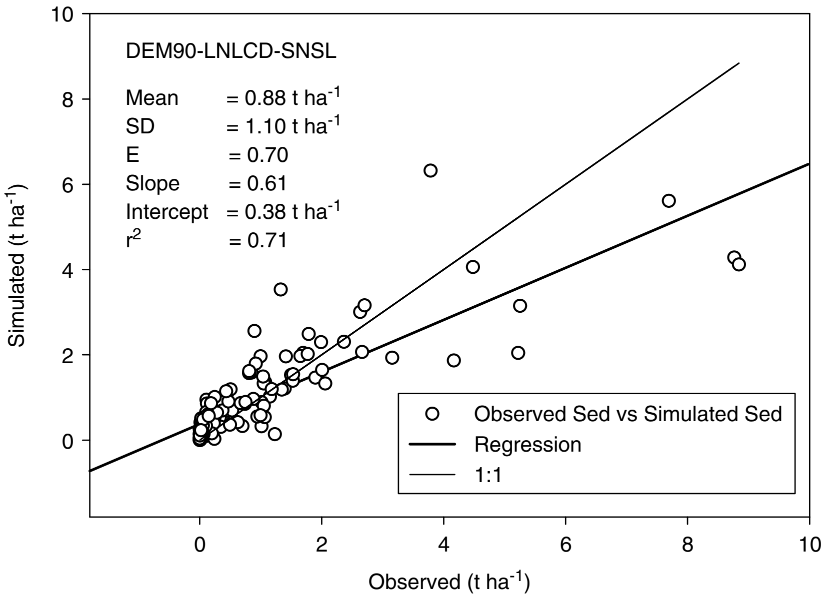


Figure 6. Observed and simulated monthly sediment yield using the GIS input: *DEM 90–LNLCD–SNLS*

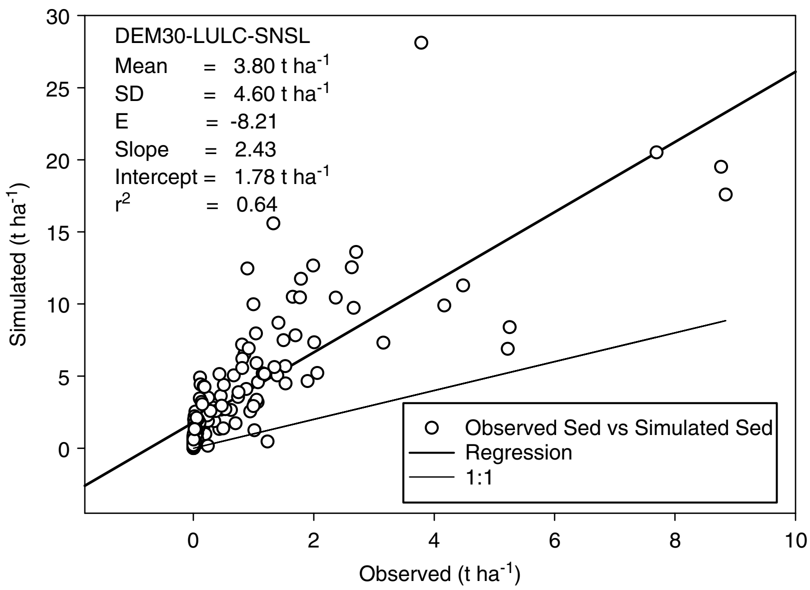


Figure 7. Observed and simulated monthly sediment yield using the GIS input: *DEM 30–LULC–SNLS*

2. The coarsest land use–land cover map (*LULC*) causes higher values of runoff output within a general underestimating context, therefore the unexpected improvement in *E* for runoff is solely connected to this issue. In addition, the distribution of this map shows that the date of collection and assumption of the land interpretation (i.e. overestimate of agriculture land) determines a conspicuous variation of the output. The issue of the subjectivity of the remote sensing interpretations is also highlighted observing the different classes and their distributions of the two Landsat 5 derived maps, as well as the mismatch of survey for

 

the year 1992 and *NLCD*. The results show that while runoff estimates are not affected, sediment yields are sensitively biased by land use map. This issue, joined to the fact that a limited number of HRUs are defined using a coarse input (i.e. *LULC*), highlights that an improper land use–land cover map can determine sensitive variations of the output as well as preventing the possible formulation of more precise and diversified management strategies related to the land use classes within small watersheds and their composing subwatersheds.

3. The coarsest soil map shows a more moderated impact on the simulations, although some input parameters (i.e. KSAT) are sensitive. A more important aspect is that a limited number of HRUs defined using a coarse soil map prevents the possible formulation of more precise and diversified management strategies related to the soil classes within small watersheds and their composing subwatersheds.
4. This study, on a small watershed scale, indicates that the GIS inputs play an important role in defining different values of sensitive input parameters of SWAT. The magnitude and direction of the variations in parameter values cannot be known *a priori* due to the complex interplay of various model components. Nevertheless, the study suggests a hierarchical importance of the GIS input: the coarsest DEM (*DEM 90*) inappropriately defines the watershed geometry, but this relevance could be less for bigger watersheds; more detailed land use–land cover maps allow us to pinpoint management strategies, if map sources (i.e. remote sensing data) are supported by timely local surveys (i.e. groundtruth); the soil map could be relevant only when a required improvement of the management strategies is associated with its units (i.e. precision agriculture).
5. AVSWAT's users may rely on available GIS data sets to make their water quality assessment at the small watershed scale, but this study highlights some useful and hidden elements that may affect assessments, particularly in ungauged situations. These issues may become relevant whenever management scenarios are compared. While a future AVSWAT system may need to include dynamic GIS layers (i.e. land use–land cover maps), there is also a need for criteria and methods to evaluate their spatial distribution and accuracy, and to estimate the associated ranges of uncertainty of the model inputs and outputs. An analysis based on the accuracy of these data was not feasible for this watershed, because precise ground surveys were not available, along with an extended and diversified spectrum of GIS data.

## CONCLUSIONS

The AVSWAT system bases the definition of the watershed hydrologic simulation schema on three fundamental GIS layers: DEM, land use–land cover and soils map. Since digital maps are becoming easily available, the objective of this study was to compare non-calibrated simulations, significant for the majority of ungauged small watersheds, using combinations of readily available GIS data.

SWAT and the ArcView interface provided reasonable results, both for total runoff and sediment yield, without calibration. The coarsest DEM, due to the inaccurate subwatershed delineation, caused a lower estimation of watershed area and a corresponding decrease in runoff. This may not be a problem at larger watershed scales. Since topographic parameters are affected, the DEM resolution causes inaccuracies for erosion and sediment yield predictions. Less detailed land use–land cover maps cause significant variations in runoff and fine sediment yields. Although the model is sensitive to soil properties, in GCW, the soils map scale did not have a relevant impact on model results.

The study highlights the inadequacy of the coarsest DEM and land use map used for a small watershed scale. Larger scale data sets, DEM and land use maps can provide sensitive improvement of the simulations. Larger scale land use and soil maps can provide a higher number of HRUs and allow the formulation of more precise and diversified management strategies related to the land use and soil classes within small watersheds and their composing subwatersheds. Fundamentally, the land use map should also be validated by ground surveys collected at the time of the simulation period.

 

Further investigations are needed to determine the role of the input GIS data sets on different watersheds, with various sizes, in varying geoclimatic and land resource regions. The derived methods could be useful when applying the SWAT and other hydrologic models at various watershed scales by targeting the uncertainty of the associated input and output variables, thereby determining the need for costly and time-consuming collection of more detailed GIS data sets in order to improve model predictions.

## ACKNOWLEDGEMENTS

We acknowledge the National Sedimentation Laboratory (NSL) of the US Department of Agriculture's Agricultural Research Service in Oxford, MS, for providing the experimental data of Goodwin Creek watershed.

## ABBREVIATIONS

| | |
|---|---|
| AVSWAT | ArcView geographical information system–SWAT model system |
| CN | SCS curve number |
| DEM | digital elevation model |
| *DEM 30* | USGS DEM, 1-arc-sec, 1 : 24 000-scale, cell size around 30 m |
| *DEM 90* | USGS DEM, 3-arc-sec, 1 : 250 000-scale, cell size around 90 m |
| *E* | simulation model efficiency (Nash and Sutcliffe, 1970) |
| HRU | hydrologic response unit |
| GCW | Goodwin Creek watershed |
| GIS | geographic information system |
| GRASS | geographic resources analysis support system GIS |
| *LNSL* | land use–land cover map provided by NSL, derived from Landsat 5 Thematic Mapper 1987, cell size 30 m |
| *LNLCD* | land use–land cover map, National Land Cover Data 1992, cell size 30 m |
| *LULC* | USGS land use–land cover map, 1 : 250 000-scale |
| MS | Mississippi state (United States) |
| MUUF | map unit user files |
| NRCS | Natural Resources Conservation Service |
| NSL | National Sedimentation Laboratory, USDA-ARS, Oxford, MS |
| SCS | Soil Conservation Service, now Natural Resources Conservation Service |
| SSURGO | Soil Survey Geographic database |
| *SNSL* | soil survey map provided by NSL |
| *STATSGO* | State Soil Geographic database |
| SWAT | Soil and Water Assessment Tool |
| TMDL | total maximum daily load |
| USDA-ARS | United States Department of Agriculture, Agriculture Research Service |
| USGS | United States Geological Survey |

## REFERENCES

Alonso CV, Bingner RL, Kuhnle RA. 1995. Sediment yield from watersheds with eroding channels. In *Water Resources Engineering*, Espey WH Jr, Combs PG (eds). ASCE **2**: 1183–1187.

Anderson JR, Hardy EE, Roach JT, Witmer RE. 1976. *A land use and land cover classification system for use with remote sensor data*. US Geological Survey Professional Paper 964, 28.

Arnold JG, Srinivasan R, Muttiah RS, Williams JR. 1998. Large area hydrologic modeling and assessment part I: model development. *Journal of American Water Resources Association* **34**(1): 73–89.

 

Arnold JG, King KW, Srinivasan R, Di Luzio M. 2002. SWAT2000: *current capabilities and research opportunities in applied watershed modeling*. 2002 ASAE Annual International Meeting, Chicago, IL, July 28–31, 2002, paper no. 022137.

Baumer O, Kenyon P, Bettis J. 1994. *MUUF v2·14 user's manual*. Natural Resource Conservation Service, National Soil Survey Center, Lincoln, NE.

Beck JM, Shaw JN, Chaney PL, Hairston JE. 2002. Image rectification for recompiling and digitizing soil survey maps. *Journal of Soil and Water Conservation* **57**(2): 95–100.

Bingner RL. 1996. Runoff simulated from Goodwin Creek Watershed using SWAT. *Transactions of the ASAE* **39**(1): 85–90.

Bingner RL, Alonso CV, Arnold JG, Garbrecht J. 1997a. Simulation of fine sediment yield within a DEC watershed. In *Management of Landscapes Disturbed by Channel Incision, Stabilization, Rehabilitation, and Restoration*, Wang SY, Langendoen E, Shields FD Jr (eds). University of Mississippi Press: Mississippi; 1106–1110.

Bingner RL, Garbrecht J, Arnold JG, Srinivasan R. 1997b. Effect of watershed subdivision on simulation runoff and fine sediment yield. *Transactions of the ASAE* **40**(5): 1329–1335.

Di Luzio M, Srinivasan R, Arnold JG, Neitsch SL. 2002. *Soil and Water Assessment Tool. ArcView GIS Interface Manual: Version 2000*. Texas Water Resources Institute TR-193, GSWRL Report 02–03, BRC Report 02–07.

FitzHugh TW, Mackay DS. 2000. Impacts of input parameter spatial aggregation on an agricultural nonpoint source pollution model. *Journal of Hydrology* **236**: 35–53.

FitzHugh TW, Mackay DS. 2001. Impacts of subwatershed partitioning on modeled source and transport-limited sediment yields in an agricultural nonpoint source pollution model. *Journal of Soil and Water Conservation* **56**(2): 137–143.

Gesch DB, Oimoen MJ, Greenlee SK, Nelson CA, Steuck M, Tyler DJ. 2002. The National Elevation Dataset. *Photogrammetric Engineering and Remote Sensing* **63**(1): 5–11.

Grissinger EH, Bowie AJ, Murphey JB. 1991. Goodwin Creek bank instability and sediment yield. In *Proceedings, Fifth Federal Interagency Sedimentation Conference*, PS32–PS39.

Haverkamp S, Srinivasan R, Frede HG, Santhi C. 2002. Subwatershed spatial analysis tool: discretization of a distributed hydrologic model by statistical criteria. *Journal of American Water Resources Association* **38**(6): 1723–1733.

Kuhnle RA, Bingner RL, Foster GR, Grissinger EH. 1996. Effect of land use changes on sediment transport in Goodwin Creek. *Water Resources Research* **32**(10): 3189–3196.

McGregor KC, Bingner RL, Bowie AJ, Foster GR. 1995. Annual and monthly variation of erosivity index in Northern Mississippi. *Transactions of the ASAE* **38**(4): 1039–1047.

Nash JE, Suttcliffe JE. 1970. River flow forecasting through conceptual models, Part I—A discussion of principles. *Journal of Hydrology* **10**(3): 282–290.

Srinivasan R, Arnold JG. 1994. Integration of a basin-scale water quality model with GIS. *Water Resources Bulletin* **30**(3): 453–462.

US Department of Agriculture, Agriculture Research Service (USDA-ARS). 1995. *Documentation of hydrologic, geomorphic, and sediment transport measurements on the Goodwin Creek experimental watershed, northern Mississippi, for the period 1982–1993*, preliminary release. Research Report 3, National Sedimentology Laboratory, Oxford, MS.

US Department of Agriculture, Soil Conservation Service (USDA-SCS). 1972. *National Engineering Handbook*, Hydrology Section 4, Chapter 4–10, 19. USDA-SCS: Washington, DC.

US Department of Agriculture, Soil Conservation Service (USDA-SCS). 1992. *State Soil Geographic Database (STATSGO) Data User's Guide*. Publication no. 1492. US Government Printing Office: Washington, DC.

US Department of Agriculture, Soil Conservation Service (USDA-SCS). 1994. Soil Survey Geographic (SSURGO) database: data use information.

US Environmental Protection Agency (USEPA). 1999. *Protocol for developing nutrient TMDLs*. Office of Water (4503F) Report EPA-841-B-99-007.

US Geological Survey (USGS), Department of the Interior. 1990. *Digital Elevation Models: Data Users Guide. National Mapping Program, Technical Instructions, Data Users Guide* 5, Reston, VA; 38.

US Geological Survey (USGS). 2003. Shuttle Radar Topography Mission. Mapping the World in 3 Dimensions; http://srtm.usgs.gov/

Vogelmann JE, Howard SM, Yang L, Larson CR, Wylie BK, Van Driel N. 2001. Completion of the 1990s National Land Cover Dataset for the conterminous United States from Landsat Thematic Mapper data and ancillary data sources. *Photogrammetric Engineering and Remote Sensing* **67**(6): 650–662.

Wilson JP, Mitasova H, Wright DJ. 2000. Water resource applications of Geographic Information Systems. *URISA Journal* **12**(2): 61–79.

 